Contrastreaming Instability in a One-Dimensional Finite-Length System

A. T. LIN AND J. E. ROWE

Electron Physics Laboratory, Department of Electrical Engineering, The University of Michigan, Ann Arbor, Michigan 48104

(Received 25 March 1971; final manuscript received 11 August 1971)

Two independent and oppositely directed electron beams with equal densities and speeds are considered to interpenetrate one another in a finite-length system with a stationary neutralizing ion background. The nonlinear development of the resulting electrostatic waves is followed both in time and space by numerical simulation. The results include the time-dependent behavior of the particle trajectories governed by the equation $W=\frac{1}{2}mv^2-|q\phi_0(t)|\cos k_{max}z$. In the cold beam case a hysteresis-like loop in phase space is observed to develop in the transition from the laminar to a turbulent state. The vortices formed in velocity space are found to be absorbed at the right-hand boundary of the finite-length system and coalesce into one another for all warm beam cases. The total electric field energy saturates at approximately 16% of the total system energy. This result is three times greater than for a one-dimensional system with periodic boundary conditions.

I. INTRODUCTION

Ever since Bernstein *et al.*[1] predicted that a stationary large-amplitude wave constituted an exact solution of the Vlasov equation for a two-component unbounded plasma, many people have tried to resolve the possible existence of such waves in practice. The development of the contrastreaming instability was investigated by Dawson[2] using a one-component charge sheet model with the initial condition of two cold electron beams interpenetrating one another. Roberts and Berk,[3] using the water-bag simulation model to study the contrastreaming instability, found that the streams relax to a vortex structure which exhibits standing nonlinear electrostatic waves predicted by Bernstein *et al.* Morse and Nielson[4] have simulated plasma ions as a neutralizing immobile background and electrons by the particle-in-cell method, and have observed the formation, coalescing, and long-time persistence of modes predicted by Bernstein *et al.* in their contrastreaming warm plasma. All of the above investigations are for a one-dimensional, unbounded plasma with periodic boundary conditions. Davis and Bers[5] employed the one-component charge sheet model to study the beam-plasma interaction in a finite-length system. They concluded that the plasma density gradients along the direction of beam drift were necessary to explain the narrow beam-velocity spread after the interaction with the plasma in their laboratory experiments.

In the present investigation we consider two independent and oppositely directed electron beams of equal densities and speeds interpenetrating one another in a stationary neutralizing ion background for a finite-length system. The nonlinear development of the resulting electrostatic waves is followed both in time and space by numerical simulation using an infinite sheet model. The stability of these nonlinear stationary waves depends on whether the nonlinearities inherent in the system and other loss mechanisms are able to suppress the growth of the waves arising from the instability. The effects of a finite-length system and particle thermal spread on the nonlinear development of the contrastreaming instability are investigated via the computer simulation. The computational method and the results of several numerical experiments are described.

II. MATHEMATICAL MODEL

The model consists, on the average, of 2600 electron sheets divided into streams with equal densities but oppositely directed mean velocities. The initial electron sheet distribution is spatially uniform with a velocity distribution (generated by a random number generator) corresponding to two equal and oppositely drifting Maxwellian streams:

$$f_0(v)=[(2\pi)^{1/2}V_{T0}]^{-1}\{\exp[-(v-V_0)^2/2V_{T0}^2]+\exp[-(v+V_0)^2/2V_{T0}^2]\}.$$

Electron sheets are injected at a fixed rate into the interaction region from opposing emitter planes and are collected whenever they reach a boundary plane. The system is approximately ten nominal wavelengths long ($2\pi V_0/\omega_{p0}$), where ω_{p0} is the total plasma frequency and V_0 is the stream mean velocity which is equal to 40 for all numerical experiments reported here. In the computations, distance is normalized to the average plasma intersheet spacing ($0.025\ V_0/\omega_{p0}$), time to $1/\omega_{p0}$, and acceleration to $0.025\ V_0\omega_{p0}$. The results are given as computer-generated plots at $5/\omega_{p0}$ time intervals. The computation is terminated at $t=40/\omega_{p0}$. Four experiments with different beam parameters will be discussed. Figure 1 shows contours of growth rate versus wavenumber calculated from the plasma dispersion equation for the parameters corresponding to the cases simulated.

III. DISCUSSION OF RESULTS

The first numerical experiment considers electron beams with zero thermal spread. In order to excite the fastest growing mode in the system, the electron

beam traveling to the right is velocity modulated with a one percent modulation depth at the total plasma frequency before it enters the interaction region. The velocity modulation is converted into charge bunching in a short distance and thereupon induces bunching in the other stream. The two beams slow down and tend to bring one another to rest, and in the process they give a portion of their streaming energies to the instability. According to linear theory (Fig. 1) the fastest growing mode in this case should occur at a wavenumber of $k_{max}=0.62\omega_{p0}/V_0$ with a growth rate of $\gamma = 0.353\,\omega_{p0}$. The results of the computer simulation (Fig. 2) give the amplitude ratio of beam acceleration at $t=20/\omega_{p0}$ to that at $t=15/\omega_{p0}$ approximately as 5.2, which yields an exponential growth rate of $\gamma=0.33\omega_{p0}$, and the fundamental mode occurs at $k\approx 0.6\omega_{p0}/V_0$;

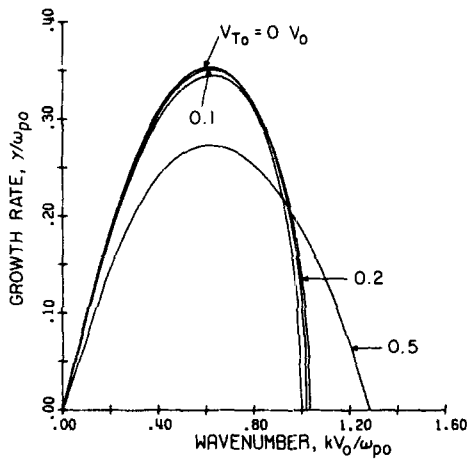

FIG. 1. Linear growth rate versus wavenumber for the contrastreaming instability.

thus, there is good agreement with the predictions of linear theory during the early stages of the instability. At a later time ($t=25/\omega_{p0}$) the growth rate drops to $0.29\omega_{p0}$ and a vortex is formed in velocity space as can be seen in Fig. 3. At this instant the beam acceleration, which is equivalent to the electric field, is rich in harmonics and those out to the sixteenth are seen to have significant amplitude.

The nonlinearity inherent in the system is apparently not strong enough to stabilize the growth of the instability and eventually the system becomes unstable. The vortex in velocity space is eventually destroyed [Fig. 3(b)]. At the same time, a great number of collective modes other than harmonics of the fastest growing modes are excited (Fig. 4) and the system eventually passes into a turbulent state. In an initial test run with 600 electron sheets, a hysteresis-like loop in velocity space (Fig. 5) clearly develops in the transition from the laminar to turbulent states. This

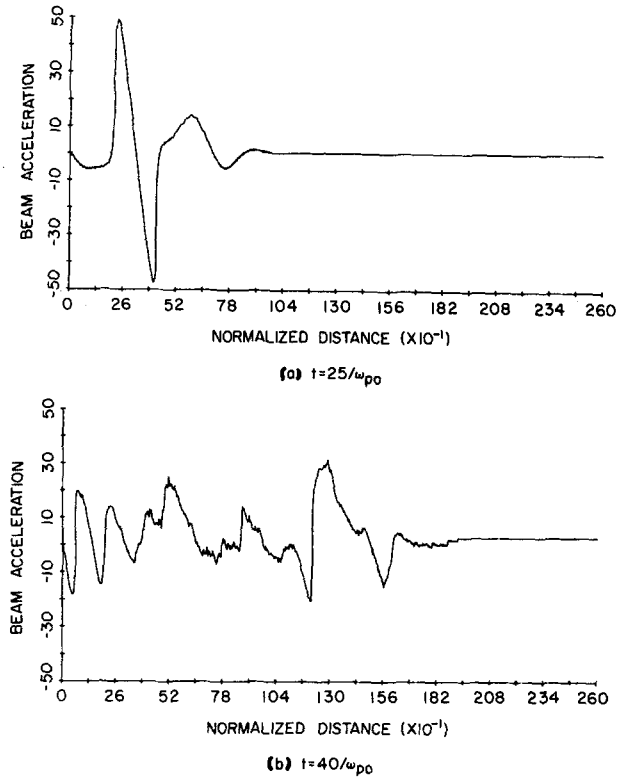

FIG. 2. Beam acceleration for the cold contrastreaming system.

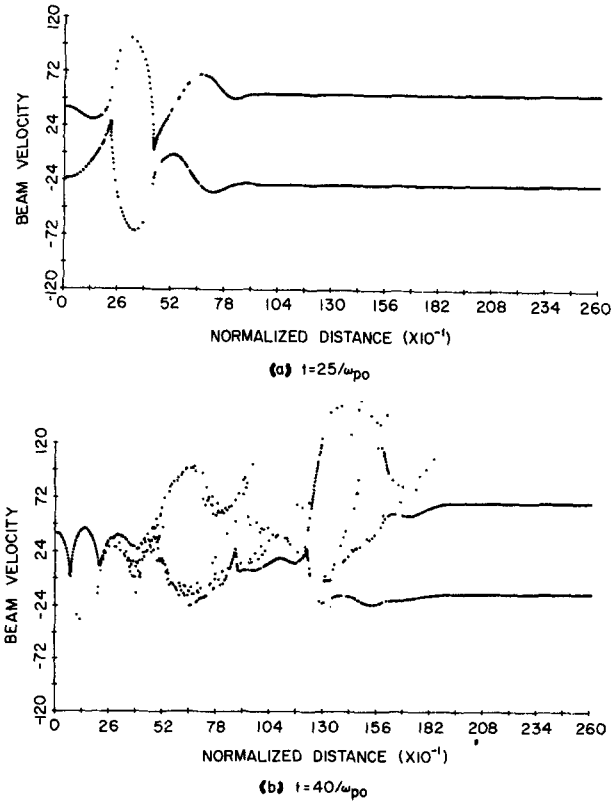

FIG. 3. Beam velocity for the cold contrastreaming system.

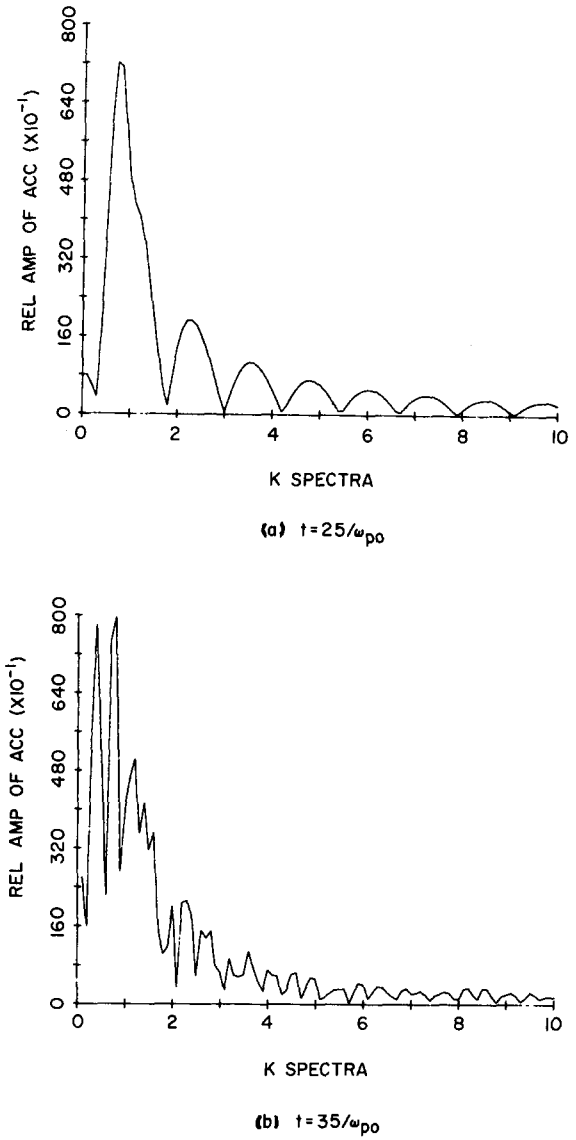

FIG. 4. Wavenumber spectrum for the cold contrastreaming system.

phenomena may be related to the "overshoot" of the contrastreaming instability. Figure 6 shows a plot of the total electrostatic field energy of the system versus time. The corresponding exponential linear growth rate at the initial stage is $\gamma=0.31\omega_{p0}$. This indicates that the field energy is concentrated in the fastest growing mode during this time interval. The field energy saturates at $t=25.7/\omega_{p0}$ when the destruction of the first vortex takes place. The field energy then levels off due to the incoherent nature of oscillations at this instant and grows again as soon as the second vortex is formed. From a comparison of Figs. 3 and 6 it is concluded that every peak in the time evolution of the field energy corresponds to the destruction of a vortex in velocity space.

Three numerical experiments are presented to illustrate the effects of beam thermal spread on the instability. In these cases, the coherent phases necessary to sustain oscillations are partly destroyed by the thermal motion of beam electrons which can carry away the oscillatory energy of the coherent oscillation and thus result in a reduction of growth rate as indicated in Fig. 1. Maxwellian velocity distributions about mean streaming velocities are generated using a random number generator so that all components of collective modes are initially excited at all locations in the system. Thermal spreads of $V_{T0}/V_0=0.1$, 0.2, and 0.5 have been investigated. The system length is approximately six wavelengths of the fastest growing mode which is defined as $\lambda_{max}=2\pi/k_{max}=\lambda_{nom}/0.6$. A sufficient relative drift between the beams will support the unstable growth of electrostatic waves in which the fastest growing mode dominates. Figures 7 and 8 show the time development of the system for the case of $V_{T0}=0.1V_0$ (four sheets per Debye length). It is apparent from the velocity space diagram that at the time $t=15/\omega_{p0}$ approximately six vortices have developed in the system. The number of vortices

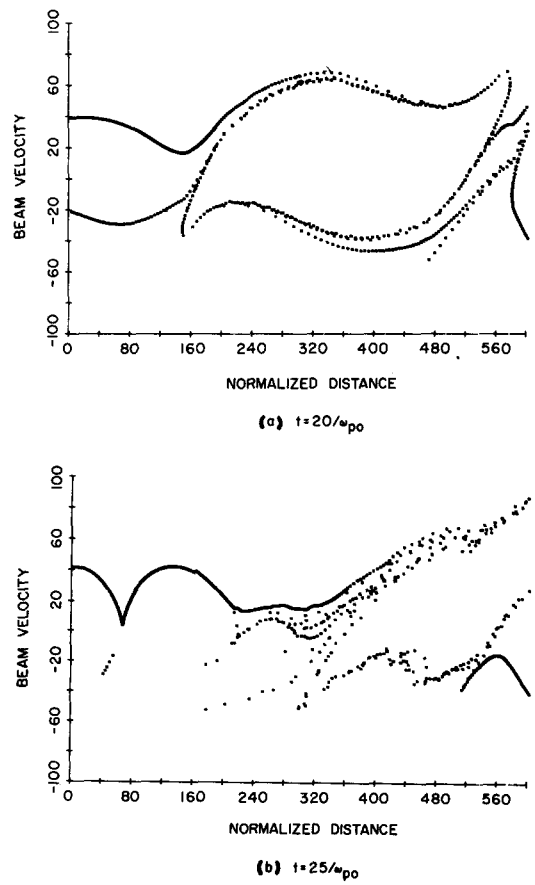

FIG. 5. Beam velocity for the cold contrastreaming system with interaction length reduced to 600 units of $0.025\ V_0/\omega_{p0}$.

formed is equal to the number of wavelengths of the mode with the largest linear growth rate fitted into the system which indicates that the vortex may be identified with the nonlinear development of the fastest growing mode with zero phase velocity. The spatial distribution of the electrostatic potential can be written as $\Phi=\Phi_0(t)\cos k_{\max}z$. The electron sheet trajectories will then be governed by the equation[6] $W=(1/2)mv^2-|q\Phi_0(t)|\cos k_{\max}z$. Figure 7 illustrates the time-dependent behavior of the trajectory equation. These velocity-distance plots indicate that the electron sheets are untrapped ($W>0$), until $t=15/\omega_{p0}$ when the electrostatic potential has grown to a sufficient amplitude to give trapped particle trajectories ($W<0$). The time evolution of the total field energy (Fig. 9) indicates an exponential growth between $t=11/\omega_{p0}$ and $t=15/\omega_{p0}$ at the rate of $\gamma=0.25\omega_{p0}$. The field energy ceases growing at approximately $t=16/\omega_{p0}$ when the

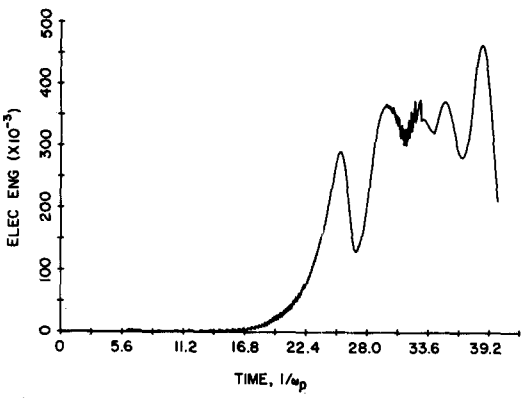

FIG. 6. Total electric field energy versus time for the cold contrastreaming system.

velocity distribution plot (Fig. 8) shows that the initially distinct beam structure has almost merged to one beam with a Maxwellian distribution. The electron beams have given up sufficient drift energy to the instability so that the beam structure is nearly destroyed.

The vortices are unstable; comparison of velocity plots at $t=15/\omega_{p0}$ and $t=25/\omega_{p0}$ shows that two vortices have coalesced into one, and another vortex has been absorbed by the right-hand boundary plane such that the number of vortices in the system at $t=25/\omega_{p0}$ is reduced to approximately four. The absorption of a velocity space vortex at the right-hand boundary can be understood as follows. The electrostatic potential developed from the instability in the system will trap some electron sheets and prohibit them from being collected by the boundaries. Since electron sheets are being continuously injected into the interaction region, the system will, on the average, possess excessive negative charges which will in turn produce an electro-

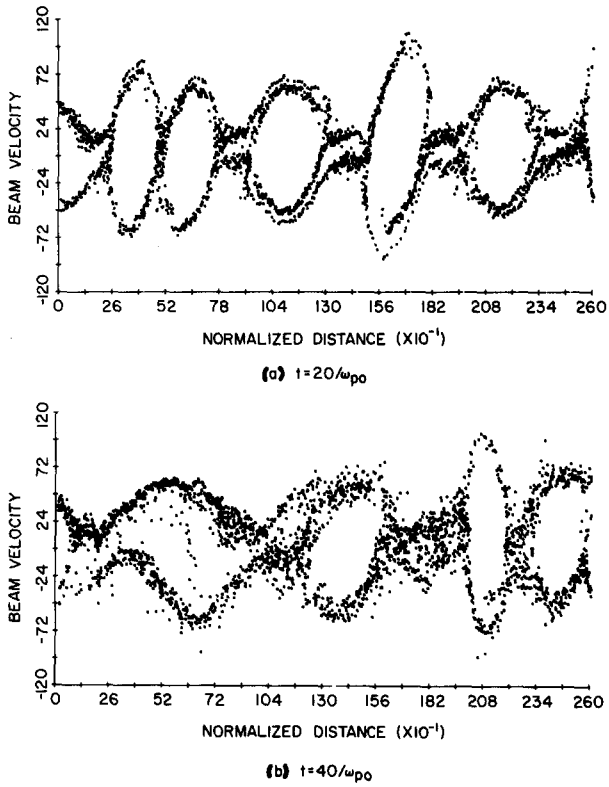

FIG. 7. Beam velocity for the warm contrastreaming system with $V_T=0.1\,V_0$.

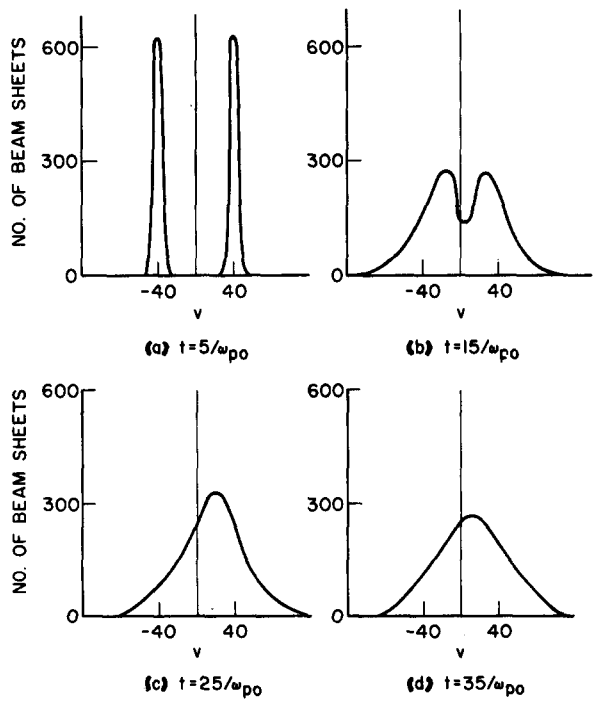

FIG. 8. Velocity distribution for the warm contrastreaming system with $V_T=0.1V_0$.

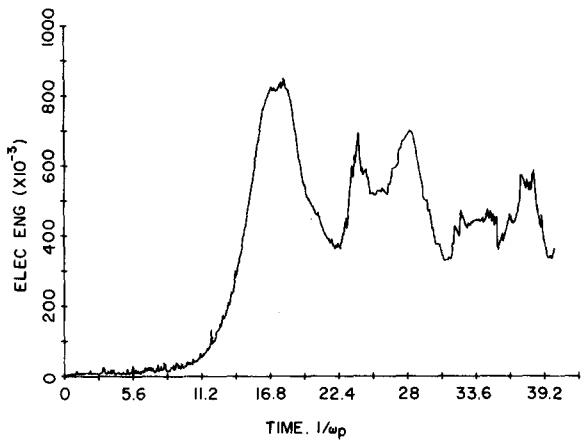

FIG. 9. Plot of total electric-field energy versus time for the warm contrastreaming system with $V_T=0.1\ V_0$.

static electric field (from Poisson's equation) in the negative direction to accelerate the electron sheets in the positive direction. The total velocity distribution will therefore acquire a drifting motion to the right as can be seen in Fig. 8. Hence, the vortex will eventually be absorbed by the right-hand boundary plane.

A further increase in thermal spread naturally decreases the instability growth rate and consequently reduces the rate of formation of vortices. Figures 10 and 11 show the velocity space evolution in time for $V_{T0}/V_0=0.2$ and 0.5, respectively. For the case shown in Fig. 11 the vortex is hardly developed at $t=30/\omega_{p0}$ due to the small growth rate of the fastest growing mode. The other characteristics of the instability remain unchanged from the previous case with $V_{T0}/V_0=0.1$.

In all experiments, the total field energy saturates at approximately 16% of the total system energy

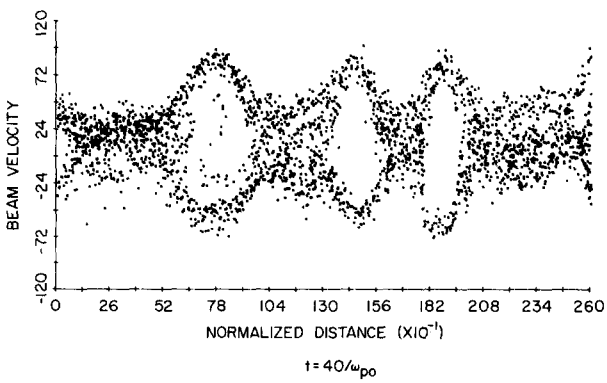

FIG. 10. Beam velocity for the warm contrastreaming system with $V_T=0.2\ V_0$.

which indicates that the finite-length effect results in a saturation energy three times as great as that reached in a system with a periodic boundary condition.[3]

IV. SUMMARY

The numerical experimental results for the contrastreaming instability in a one-dimensional finite-length system demonstrate that the velocity space vortices in a cold system are unstable with respect to the nonlinearity, whereas in a warm system the vortices persist for a long time because the thermal spread reduces the growth rate. The vortices are observed to be absorbed at the right-hand boundary plane and coalesce into one another in all warm beam cases. The phase-space plots also display the trapped and

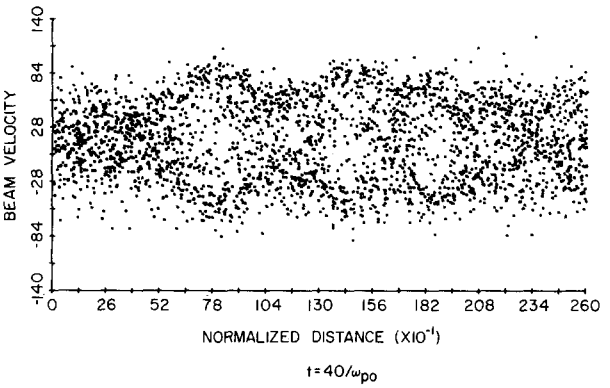

FIG. 11. Beam velocity for the warm contrastreaming system with $V_T=0.5\ V_0$.

untrapped situations for the electron sheet trajectory equation. The assumption of a finite-length system leads to an electric-field energy three times that found when periodic boundary conditions are assumed.

ACKNOWLEDGMENT

The authors acknowledge support from the National Science Foundation Grant No. GK-15689.

[1] I. B. Bernstein, J. M. Greene, and M. D. Kruskal, Phys. Rev. **108**, 546 (1957).
[2] J. Dawson, Nucl. Fusion Suppl. Pt. 3, 1033 (1962).
[3] K. V. Roberts and H. L. Berk, Phys. Rev. Letters **19**, 297 (1967).
[4] R. L. Morse and C. W. Nielson, Phys. Rev. Letters **23**, 1087 (1969).
[5] J. A. Davis and A. Bers, in *Proceedings of the Symposium of Turbulence of Fluids and Plasmas* (Polytechnic Press of the Polytechnic Institute of Brooklyn, Brooklyn, New York, 1968), p. 87.
[6] R. Z. Sagdeev and A. A. Galeev, *Nonlinear Plasma Theory* (Benjamin, New York, 1969), p. 38.